Interaction of $G\alpha_{12}$ with $G\alpha_{13}$ and $G\alpha_q$ signaling pathways

Jennifer L. Gu*†, Stefan Müller*‡, Valeria Mancino†, Stefan Offermanns§, and Melvin I. Simon†¶

†Division of Biology, 147-75 California Institute of Technology, Pasadena, CA 91125; ‡Axxima Pharmaceuticals AG, Am Klopferspitz 19, 82152 Martinsried, Germany; and §Pharmakologisches Institut, Universität Heidelberg, Im Neuenheimer Feld 366, 69120 Heidelberg, Germany

Contributed by Melvin I. Simon, May 15, 2002

The G_{12} subfamily of heterotrimeric G-proteins consists of two members, G_{12} and G_{13}. Gene-targeting studies have revealed a role for G_{13} in blood vessel development. Mice lacking the α subunit of G_{13} die around embryonic day 10 as the result of an angiogenic defect. On the other hand, the physiological role of G_{12} is still unclear. To address this issue, we generated $G\alpha_{12}$-deficient mice. In contrast to the $G\alpha_{13}$-deficient mice, $G\alpha_{12}$-deficient mice are viable, fertile, and do not show apparent abnormalities. However, $G\alpha_{12}$ does not seem to be entirely redundant, because in the offspring generated from $G\alpha_{12}\pm$ $G\alpha_{13}\pm$ intercrosses, at least one intact $G\alpha_{12}$ allele is required for the survival of animals with only one $G\alpha_{13}$ allele. In addition, $G\alpha_{12}$ and $G\alpha_{13}$ showed a difference in mediating cell migratory response to lysophosphatidic acid in embryonic fibroblast cells. Furthermore, mice lacking both $G\alpha_{12}$ and $G\alpha_q$ die *in utero* at about embryonic day 13. These data indicate that the $G\alpha_{12}$-mediated signaling pathway functionally interacts not only with the $G\alpha_{13}$- but also with the $G\alpha_{q/11}$-mediated signaling systems.

Heterotrimeric G proteins transduce a variety of signals generated by the interaction of hormones, growth factors, neurotransmitters, odorants, or photons, with cell surface receptors. On the basis of sequence similarities of the α subunits, G proteins were grouped into four subfamilies: G_s, $G_{i,o}$, G_q, and G_{12} (1). Members of the G_{12} subfamily, $G\alpha_{12}$ and $G\alpha_{13}$, are ubiquitously expressed and share 67% amino acid identity (2). Receptors that respond to a variety of ligands, such as those for thrombin, thromboxane A_2, lysophosphatidic acid (LPA), sphingosine 1-phosphate, thyroid-stimulating hormone, bradykinin, endothelin, neurokinin A, and angiotensin AT_{1A}, have been shown to couple to $G\alpha_{12}$ and/or $G\alpha_{13}$ (3–11). Both the activated forms of $G\alpha_{12}$ and $G\alpha_{13}$, $G\alpha_{12}$Q229L and $G\alpha_{13}$Q229L, were found to cause transformation of fibroblasts (12–14), to activate the JNK pathway (15, 16), to activate the serum response element (17, 18), and to regulate different isoforms of Na^+H^+ exchangers (19–22). Activated $G\alpha_{12}$ and $G\alpha_{13}$ lead to stress fiber formation/focal adhesion assembly in Swiss 3T3 cells (23) and to neurite retraction in PC-12 cells (24). In addition, $G\alpha_{12}$ and $G\alpha_{13}$ have been shown to activate phospholipase-D (25, 26) as well as the transcription of cyclooxygenase-2 (27) and Egr-1, a primary response gene implicated in cell proliferation (28). The small GTPases Ras, Rac, CDC42, and especially RhoA seem to play a critical role in $G\alpha_{12}$ and $G\alpha_{13}$ signaling processes. Regulatory molecules such as RhoA-specific guanine nucleotide exchange factors p115RhoGEF (GEF, guanine nucleotide exchange factor) and PDZ-RhoGEF, and the GTPase-activating protein RasGAP1 were found to mediate some of these effects by a direct interaction with $G\alpha_{12}$ and $G\alpha_{13}$ (29–31). Furthermore, the G_{12} family proteins have been shown to activate tyrosine kinases, including epidermal growth factor receptor tyrosine kinase (32), Tec/Bmx kinases (33), focal adhesion kinase (FAK) (34), and Pyk-2 (35).

In many experiments, particularly transfection experiments, $G\alpha_{12}$ and $G\alpha_{13}$ showed mostly overlapping functions when dominant active mutant forms were used. However, $G\alpha_{12}$ and $G\alpha_{13}$ seem to differ in their ability to couple to different ligands as well as to activate tyrosine kinase. For example, LPA apparently activates stress fiber formation through a $G\alpha_{13}$-mediated process involving epidermal growth factor receptor (EGFR) transactivation, whereas $G\alpha_{12}$ seems to mediate the stress fiber formation on thrombin stimulation, without the participation of EGFR (24, 32). It was also demonstrated that $G\alpha_{12}$ and $G\alpha_{13}$ recruit different signaling pathways to activate Na^+/H^+ exchangers (19). In addition, $G\alpha_{12}$ and $G\alpha_{13}$ seem to signal to RhoA through different pathways. The RhoA guanine–nucleotide exchange factor p115RhoGEF bound to and acted as a GTPase-activating protein for both $G\alpha_{12}$ and $G\alpha_{13}$; however, its activity as a GEF was activated only by $G\alpha_{13}$, but not $G\alpha_{12}$ (36). Furthermore, $G\alpha_{12}$ appears to have a much stronger ability to induce transformation compared with $G\alpha_{13}$, whereas $G\alpha_{13}$ leads to more severe apoptosis in COS7 cells (12, 13, 37–39). These data suggest that $G\alpha_{12}$ and $G\alpha_{13}$ have similar activities with respect to some functions but are nevertheless readily distinguishable with respect to other functions.

In recent years, gene targeting experiments in mice have been used to learn more about the physiological role of G proteins. The absence of $G\alpha_{13}$ resulted in impaired angiogenesis and intrauterine death at day 10. We have now generated mice deficient for $G\alpha_{12}$. In contrast to the $G\alpha_{13}$-deficient animals, the $G\alpha_{12}$-knockout mice are alive and show no apparent phenotype. However, crossbreeding with mice carrying a mutation in the $G\alpha_{13}$ or $G\alpha_q$ gene suggests that $G\alpha_{12}$ has a role in mouse embryogenesis, and that it functionally interacts with signaling pathways using both $G\alpha_{13}$ and $G\alpha_q$.

Materials and Methods

Generation of $G\alpha_{12}$-Deficient Mice. A genomic clone containing exons 3 and 4 of the $G\alpha_{12}$ gene was isolated from 129/Sv mouse λ phage library (Stratagene) (40). To generate the targeting construct, a 701-bp *Xho*I–*Hpa*I fragment of exon 4 encoding the C-terminal 127 amino acids was replaced by the *Pgk*::*Neo* gene in the reverse orientation. The short arm of the targeting construct consisted of a 2-kb *Hpa*I–*Xho*I fragment, and the long arm consisted of a 4.5-kb *Afl*II–*Hpa*I fragment. The targeting construct was introduced into the CJ7 mouse embryonic stem (ES) cell line by electroporation, and the resulting G418-resistant clones were screened with a 0.9-kb *Bam*HI–*Hpa*I probe located upstream of the short arm for correct integration into the genome by Southern blot analysis. ES cells with the null mutation in one $G\alpha_{12}$ allele were injected into C57BL/6 blastocysts, and chimeras were bred with C57BL/6 and 129/Sv mice to generate heterozygous mice. Further intercrosses of the heterozygous mice produced homozygous $G\alpha_{12}$-deficient mice.

Western Analysis. Proteins for Western analysis were prepared from mouse brains (41). Samples were separated by SDS/PAGE and blotted onto nitrocellulose membranes BA85 (Schleicher &

Abbreviations: LPA, lysophosphatidic acid; MEF, mouse embryonic fibroblasts; E*n*, embryonic day *n*; ES, embryonic stem; GEF, guanine nucleotide exchange factor.

*J.L.G. and S.M. contributed equally to this work.

¶To whom correspondence should be addressed. E-mail: simonm@its.caltech.edu.

 www.pnas.org/cgi/doi/10.1073/pnas.102291599

Schüll). $G\alpha_{12}$ was detected by the N-terminal-specific polyclonal antibody S-20 (1:300, Santa Cruz Biotechnology) or by the C-terminal antiserum AS233 (1:300).

Immunohistochemistry Analysis. Embryos were isolated from uteri at embryonic days (E)8.25 and 9.5, fixed for 24 h in 4% paraformaldehyde, then transferred to methanol via consecutive steps of increasing methanol concentrations and stored at −20°C. Whole-mount immunohistochemical staining of mouse embryos with antiplatelet–endothelial cell adhesion molecule (PECAM)-1 monoclonal antibodies was performed as described (42). Briefly, E9.5 embryos were blocked for 2 h at reverse transcription in PBS/2% nonfat dry milk/0.2% Triton X-100 and incubated with rat anti-mouse-PECAM-1 monoclonal antibody, cl. 13.3 (0.5 mg/ml, 1:300, PharMingen) followed by affinity purified goat anti-rat alkaline phosphatase-conjugated IgG (0.3 mg/ml, 1:200, The Jackson Laboratory). The embryos were then washed with alkaline phosphatase buffer (0.1 M Tris·HCl, pH 9.5/0.1 M NaCl/50 mM $MgCl_2$/0.1% Tween 20) including 2 mM levamisole and stained in the same buffer with 350 μg/ml of nitro-blue tetrazolium and 175 μg/ml of 5-bromo-4-chloro-3-indoyl phosphate.

Mouse Embryonic Fibroblast (MEF) Cells and Retroviral Transduction. MEF cells were isolated from E8.0 $G\alpha_{12}-/-G\alpha_{13}-/-$ embryos or E9.5 $G\alpha_{13}-/-$ embryos, as described (43). Cells were maintained and passaged through crisis in DMEM (GIBCO/BRL) supplemented with 10% FBS and 180 μg (active component)/ml G418. The retroviral gene delivery system was a generous gift from Carlos Lois (California Institute of Technology). Mouse $G\alpha_{12}$ and $G\alpha_{13}$ cDNA was cloned into pBabe-puro retroviral vector. To produce retrovirus, BOSC packaging cells were transfected with retroviral constructs as described (44). Virus was collected 48 h later and centrifuged for 5 min at 1,500 × *g* to remove cells. Supernatant was aliquoted and frozen at −80°C. MEF cells grown in 6-cm plates to about 60% confluent were infected with 4 ml of the viral supernatant for 5 h, and permanent $G\alpha_{12}$ or $G\alpha_{13}$ lines were generated by selection in 2 μg/ml of puromycin 72 h post-infection.

Cell Migration Assays. Cell migration assays were performed by using Transwell migration chambers (24 wells with pore size 8 μm; Costar). MEF cells were trypsinized to obtain single-cell suspension and washed twice in migration medium (DMEM containing 0.5% fatty acid-free BSA). Cells were then resuspended in this medium at 1×10^6 cells/ml, and 100 μl of this suspension was placed in the upper compartment of the Transwell chamber. Six hundred microliters of migration media or migration media containing 5 μM LPA was placed in the lower chamber. The chambers were incubated for 4 h at 37°C in a humidified incubator with 5% CO_2 to allow cell migration. After the incubation period, the filter was removed, and the upper side of the filters was wiped gently with a cotton applicator to remove nonmigrated cells. The filters were fixed and stained with a Giemsa solution (Diff-Quick, Dade Behring AG). Migration was quantitated by counting cells that had migrated to the lower surface of the filter. Five random fields in each filter were counted. Each experiment was performed in triplicate, and migration was documented as the average number ± SD of total cells counted per field. Final results were expressed as the fold increase over the migration of noninfected cells measured at the same time. Experiments were repeated at least three times. Background cell migration (0.5% fatty acid free BSA only) was less than 5% of stimulated values.

Results

$G\alpha_{12}$ Gene-Targeted Animals Develop Normally and Show No Apparent Morphological or Behavioral Abnormalities. $G\alpha_{12}$-deficient mice were generated by targeted disruption of the $G\alpha_{12}$ gene in ES cells. The mutation was generated by replacing an *Xho*I–*Hpa*I fragment of exon 4 with the Neo gene through homologous recombination, which led to the removal of approximately one-third of the protein-coding sequence (Fig. 1*A*). ES cells carrying the deleted gene were identified by Southern analysis, and chimeric mice were obtained by injecting the 129/Sv-derived heterozygous ES cells into C57BL/6 blastocysts. Germ-line-transmitting chimeric male mice were crossed with females of both 129Sv and C57BL/6 backgrounds. More than 350 mice from $G\alpha_{12}\pm$ intercrosses were analyzed, and the distribution of genotypes was Mendelian (Table 1), suggesting that all of the possible genotypes showed normal levels of survival. Both heterozygous and homozygous $G\alpha_{12}$ mutant mice were fertile and did not show apparent morphological or behavioral abnormalities.

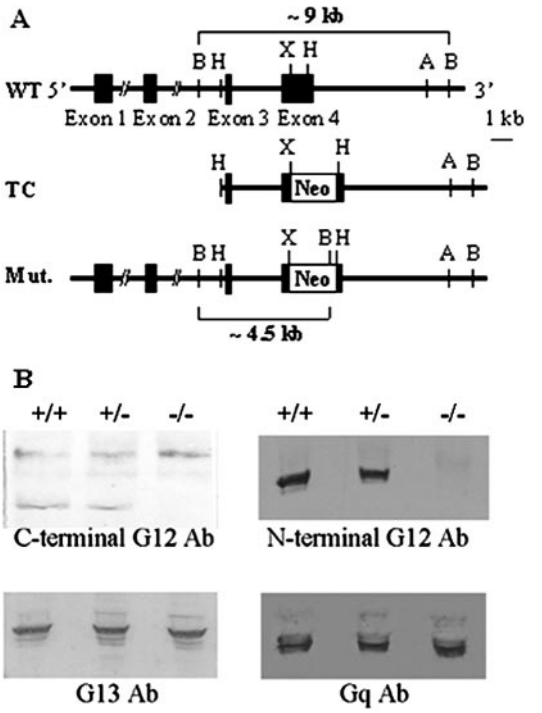

Fig. 1. Targeted inactivation of the murine $G\alpha_{12}$ gene. (*A*) Genomic structure of murine $G\alpha_{12}$ gene (WT), targeting construct (TC), and replaced mutant allele (Mut.), as described in *Materials and Methods*. (*B*) Western analysis of $G\alpha_{12}$ mice. Cholate extracts from mouse brain were used for detection by Western analysis. An approximately 45-kDa band representing $G\alpha_{12}$ was seen in wild-type tissue with antibodies against the N (N-20, Santa Cruz Biotechnology) and C termini (AS 233). Expression of $G\alpha_{13}$ and $G\alpha_q$ was also examined in both wild-type and $G\alpha_{12}$ mutant mice.

To confirm the absence of $G\alpha_{12}$ expression in mutant mice, we carried out detailed analysis at both mRNA and protein levels. Reverse transcription–PCR and Northern analysis confirmed the presence of the shortened $G\alpha_{12}$ gene transcript (data not shown). At the protein level, antibodies directed against both the N and the C termini of $G\alpha_{12}$ protein showed the absence of reactive protein (Fig. 1*B*). The lower areas of the Western blot

Table 1. Offspring of $G\alpha_{12}+/-$ intercrosses

$G\alpha_{12}$	129/Sv	C57BL/6J
+/+	16 (22.5%)	74 (27%)
+/−	44 (62%)	147 (53%)
−/−	11 (15.5%)	57 (20%)
Total	71	278

Table 2. Offspring of $G\alpha_{12}+/-G\alpha_{13}+/-$ intercrosses

$G\alpha_{12}$	$G\alpha_{13}$	E8.25	E8.5	E9.5	E10.5	P30	Predicted
+/+	+/−	4	2	4	1	18	6.25%
+/+	+/−	14	11	28	4	45	12.5%
+/+	−/−	4	2	15*	0	0	6.25%
+/−	+/+	4	8	16	2	44	12.5%
+/−	+/−	18	29	63	8	44	25.0%
+/−	−/−	9	7	25*	0	0	12.5%
−/−	+/+	4	4	10	1	24	6.25%
−/−	+/−	10	15	27*	0	0	12.5%
−/−	−/−	5	6*	0	0	0	6.25%
Total		72	85	188	16	172	

P30, postnatal day 30.
*Signs of resorption observed.

were also examined and no indication of the presence of a truncated form was observed. Even in the unlikely event that a short form were to be produced, it would be likely to be unstable and to not contain the folded portion of the protein required for the formation of a functional guanine nucleotide-binding pocket. We conclude that these mutant mice are devoid of functional $G\alpha_{12}$ protein.

$G\alpha_{12}$ Interacts with $G\alpha_{13}$ During Mouse Embryonic Development. $G\alpha_{12}$ is coexpressed with the other member of the $G\alpha_{12}$ family protein $G\alpha_{13}$ in all tissues tested so far and has been shown in many cases to have overlapping function with $G\alpha_{13}$. $G\alpha_{13}$ deficiency is characterized by a severe angiogenic defect leading to embryonic death at E10 (42). The lack of phenotype in $G\alpha_{12}$ gene-targeted mice could result from the compensation for $G\alpha_{12}$ activity by other $G\alpha$ proteins, specifically $G\alpha_{13}$. To examine this possibility, we first compared brain extracts from wild-type and $G\alpha_{12}$-deficient mice for expression levels of $G\alpha_{13}$ and $G\alpha_q$ by using specific antisera and semiquantitative immunoblot analysis (Fig. 1*B*). No significant change in expression of these α subunits was observed. To further test their genetic interactions, $G\alpha_{12}-/-$ and $G\alpha_{13}\pm$ mice were crossed to produce $G\alpha_{12}\pm G\alpha_{13}\pm$ heterozygotes, which are viable and fertile. Double heterozygotes [$G\alpha_{12}(\pm);G\alpha_{13}(\pm)$] were then intercrossed to generate offspring with different combinations of $G\alpha_{12}$ and $G\alpha_{13}$ genes (Table 2). At E8.25 (about the eight-somite stage; Fig. 2*A*), $G\alpha_{12}-/-G\alpha_{13}-/-$ embryos seem to be arrested. $G\alpha_{12}\pm G\alpha_{13}-/-$ embryos have about two to four somites. Both types of embryos show clear developmental retardation. Embryos with all other genotypes are indistinguishable from their wild-type littermates at this stage. At E9.5 (Fig. 2*B*), almost all $G\alpha_{12}-/-G\alpha_{13}-/-$embryos are either resorbed or show severe necrosis. Most of the $G\alpha_{12}\pm G\alpha_{13}-/-$ embryos show severe signs of degeneration and are in the process of being resorbed. Consistent with our previous report (42), at this stage, $G\alpha_{12}+/+G\alpha_{13}-/-$ embryos are obtained alive with signs of the development of degenerative vascular structure. These embryos contain 12–14 pairs of somites and are arrested in the turning process. Embryos with genotypes of G12±G13± and G12−/−G13+/+ are phenotypically the same as their wild-type littermates. G12−/−G13± embryos are never found at E10.5 (Table 2). The fact that in the absence of a $G\alpha_{12}$ allele, one $G\alpha_{13}$ allele is not sufficient for survival suggests that there is some functional interaction between these two genes. Interestingly, at E9.5, most $G\alpha_{12}-/-G\alpha_{13}\pm$ embryos show slightly retarded phenotypes (Fig. 2*B*). We have occasionally found $G\alpha_{12}-/-G\alpha_{13}\pm$ embryos with phenotypes indistinguishable from wild-type as well as $G\alpha_{13}-/-$ embryos (picture not shown), suggesting background genes may modify the $G\alpha_{12}$/$G\alpha_{13}$ signaling pathway. The functions of $G\alpha_{12}$ and Gα13 appear

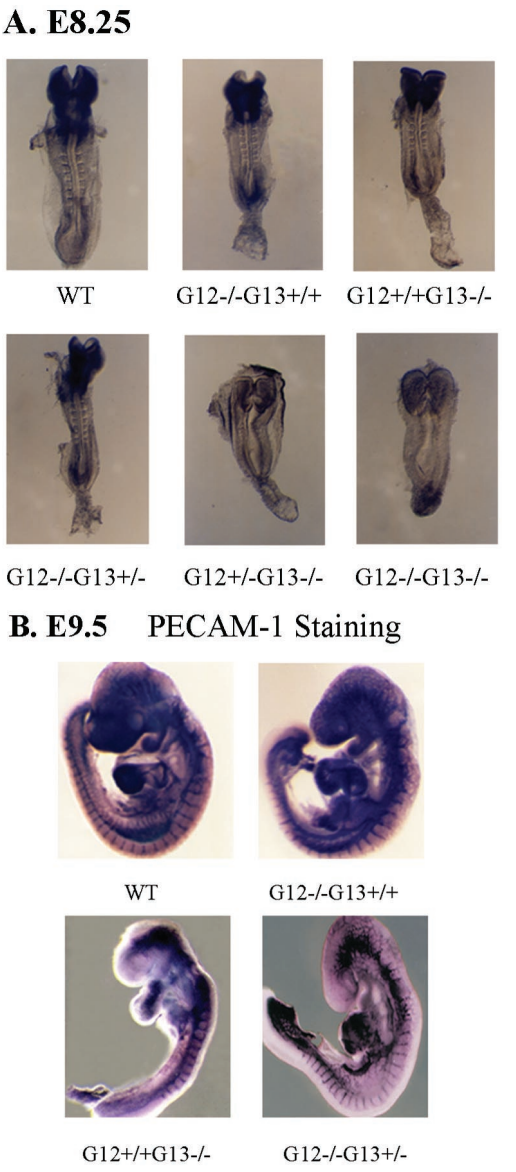

Fig. 2. Embryos from offspring of $G\alpha_{12}\pm G\alpha_{13}\pm$ intercrosses. (*A*) Embryos taken at E8.25. (*B*) Whole-mount staining of E9.5 embryos with antiplatelet–endothelial cell adhesion molecule-1 antibody (PharMingen).

to interact as suggested by the fact that embryos lacking both $G\alpha_{12}$ and $G\alpha_{13}$ die about 1 day earlier than $G\alpha_{12}+/+G\alpha_{13}-/-$ mice (Fig. 2*A*, Table 2). Taken together, these data indicate that the functions of $G\alpha_{12}$ and $G\alpha_{13}$ are partially overlapping during embryonic development. Nonetheless, in the presence of a full complement of wild-type $G\alpha_{13}$ alleles, the animals can develop even if both $G\alpha_{12}$ alleles are disrupted.

$G\alpha_{12}$ and $G\alpha_{13}$ Differ in Their Ability to Mediate LPA-Stimulated Cell Migration. We previously showed that $G\alpha_{13}$ mediates thrombin-stimulated cell migration using primary MEFs derived from wild-type and $G\alpha_{13}-/-$ embryos (42). To reduce the large variations observed in these experiments that could be due to different genetic backgrounds, we decided to examine in more detail the migratory effects of $G\alpha_{12}$ and $G\alpha_{13}$ in stable cell lines. $G\alpha_{13}-/-$ and $G\alpha_{12}-/-G\alpha_{13}-/-$ MEFs were prepared and passaged through crisis as described in *Materials and Methods.* Retrovirus-carrying $G\alpha_{12}$, $G\alpha_{13}$, and green fluorescent protein (GFP) were used to infect the cells, and stable lines expressing

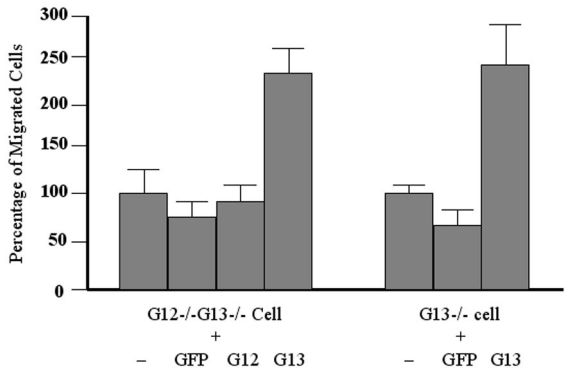

Fig. 3. LPA-induced cell migration. GFP, $G\alpha_{12}$, and $G\alpha_{13}$ expressing $G\alpha_{13}-/-$ and $G\alpha_{12}-/-G\alpha_{13}-/-$ cell lines were established by using the retroviral expression system as described in *Materials and Methods*. Migration experiments were performed in triplicate by using 24-well Transwell migration chambers, and migrated cells were quantitated in five random fields and expressed as a percentage of the control cells (−) that are always run at the same time. Two different G13−/− lines and two different G12−/−G13−/− lines were examined and showed similar results in at least two independent experiments.

$G\alpha_{13}$, $G\alpha_{12}$, and GFP were established by selection in puromycin. Expression of $G\alpha_{13}$ and $G\alpha_{12}$ was examined by Western analysis or reverse transcription–PCR (data not shown). We confirmed the role of $G\alpha_{13}$ in mediating thrombin-stimulated cell migration in $G\alpha_{13}-/-$ cells (data not shown). In addition, we observed a clear role of $G\alpha_{13}$ in mediating LPA-stimulated cell migration (Fig. 3) [the trend was observed before, although not statistically significant (42)]. Furthermore, in $G\alpha_{13}$, $G\alpha_{12}$, and GFP-expressing $G\alpha_{12}-/-G\alpha_{13}-/-$ cells, although $G\alpha_{13}$ was shown to mediate LPA-stimulated cell migration, $G\alpha_{12}$ expression did not seem to affect the migratory ability of the cells (Fig. 3). These results were observed in two different lines of $G\alpha_{13}-/-$ and $G\alpha_{12}-/-G\alpha_{13}-/-$ MEFs. They clearly demonstrated a different role for $G\alpha_{12}$ and $G\alpha_{13}$ in mediating LPA-stimulated cell migration.

$G\alpha_{12}$ Interacts with $G\alpha_q$ During Mouse Embryonic Development. Further evidence for a function for the $G\alpha_{12}$ gene product comes from crosses of $G\alpha_{12}$- with $G\alpha_q$-deficient animals. Consistent with our previous report (45), newborn $G\alpha_q$-deficient mice occasionally suffer from overt intraabdominal bleeding, which can lead to perinatal death, and $G\alpha_q-/-G\alpha_{12}+/+$ and $G\alpha_q-/-G\alpha_{12}\pm$ mice have a lower survival rate than expected at postnatal day 30 (Table 3). In addition, the $G\alpha_q$ and $G\alpha_{12}$ doubly deficient animals appear to be normal up to E12.5 but show clear signs of retardation and beginning resorption at E13.5

Table 3. Offspring of $G\alpha q+/-G\alpha 12+/-$ intercrosses

Gαq	Gα12	E11.5	E13.5	P30	Predicted
+/+	+/+	1	1	19	6.25%
+/+	+/−	4	3	19	12.5%
+/+	−/−	10	1	16	6.25%
+/−	+/+	0	3	23	12.5%
+/−	+/−	11	8	47	25.0%
+/−	−/−	13	0	42	12.5%
−/−	+/+	1	1	4	6.25%
−/−	+/−	5	2	6	12.5%
−/−	−/−	10	3*	0	6.25%
Total		55	22	176	

P30, postnatal day 30.
*Signs of resorption observed.

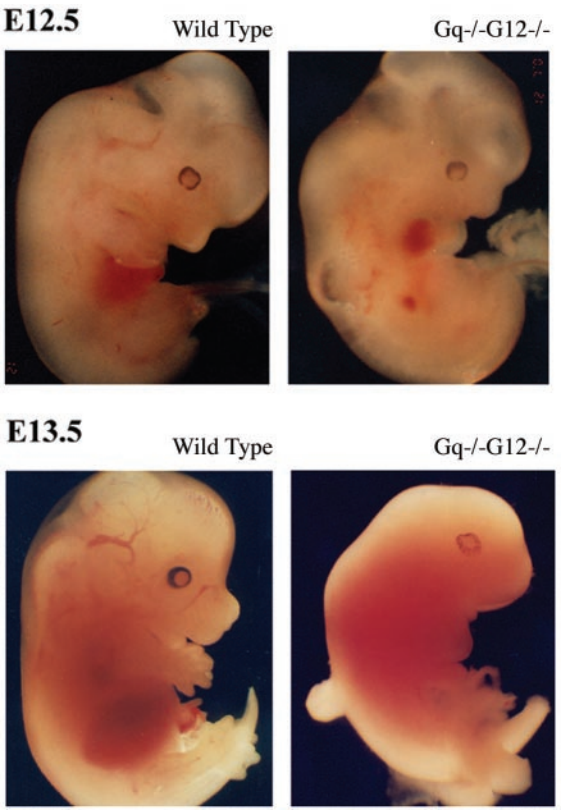

Fig. 4. Embryos from offspring of $G\alpha_q\pm G\alpha_{12}\pm$ intercrosses. (*A*) Embryos taken at E12.5. (*B*) Embryos taken at E13.5.

(Fig. 4). In contrast, most $G\alpha_q-/-$ embryos and almost all $G\alpha_{12}-/-$ embryos survive. At E12.5, both wild-type and $G\alpha_q-/-G\alpha_{12}-/-$ embryos seem to have normally developed heads, eyes, hearts, and vascular systems. Their hand- and footplates are paddle-shaped. At E13.5, in the front of the facial region of the wild-type embryo, mouth and nose are protruded. The distal borders of the hand- and footplates of the limbs are now indented, and the definitive location and width of the digits are clearly seen. However, for $G\alpha_q-/-G\alpha_{12}-/-$ embryos, the hand- and footplates are still paddle-shaped. Their development seems to stop around E12.5, and embryos show clear signs of degeneration at E13.5. These results suggest an overlapping function of $G\alpha_{12}$ with $G\alpha_q$ that is required for development and is manifested at about E12.5. Although we still do not know the details of their function, we have observed that, whereas $G\alpha_{12}$ alone is dispensable, $G\alpha_{12}$ clearly interacts with other G-protein-mediated pathways, as demonstrated in doubly deficient animals.

Discussion

In this study, we have generated mice deficient for $G\alpha_{12}$. The $G\alpha_{12}$-deficient mice are normal and show no obvious abnormalities regarding growth, rudimentary behavior, development of immune system (normal T and B cell development), or fertility. The effects of removing the $G\alpha_{12}$ gene in mice are in sharp contrast to the outcome of its close relative, $G\alpha_{13}$. $G\alpha_{13}$ deficiency in mice results in embryonic lethality at E10 due to impaired angiogenesis in both yolk sac and embryo proper with enlarged and disorganized blood vessels in the head mesenchyme (42). The generation of mice deficient for both $G\alpha_{12}$ and $G\alpha_{13}$, however, revealed that $G\alpha_{12}$ has a distinct biological function in mouse embryonic development. Embryos with $G\alpha_{12}$ and $G\alpha_{13}$ double deficiency die between E8 and E8.5. Embryos carrying only one $G\alpha_{12}$ allele ($G\alpha_{12}\pm G\alpha_{13}-/-$) survive a little

longer and die around E9.0. The presence of a single allele of $G\alpha_{13}$ in combination with a single $G\alpha_{12}$ allele is sufficient to provide survival. However, in the absence of a $G\alpha_{12}$ allele, one $G\alpha_{13}$ allele is not sufficient for survival (Table 2). These results suggest that $G\alpha_{12}$ has an overlapping as well as distinct function with $G\alpha_{13}$ in early mouse development.

$G\alpha_{12}$ and $G\alpha_{13}$ doubly deficient embryos at E8.25 have a poorly developed headfold, no somites, and unclosed and sometimes kinked neural tubes (Fig. 2*A*). The allantois is short and thick and not fused to the chorion. All these features resemble closely the phenotypes observed in mice deficient for genes involved in cell migration and cell adhesion such as fibronectin, p125FAK, or vinculin (46–49), and are consistent with evidence for a pivotal role for $G\alpha_{12}$ and $G\alpha_{13}$ in mediating signals leading to cytoskeleton rearrangement and extracellular matrix adhesion. For example, LPA that causes rearrangements of the actin cytoskeleton via the G12 subfamily induces enhanced binding of fibronectin to cells (50). Moreover, leukocyte adhesion to endothelial cells via certain integrins is Rho-dependent (51) and might also involve $G\alpha_{12}$ or $G\alpha_{13}$. Finally, active forms of $G\alpha_{12}$ and $G\alpha_{13}$ lead to phosphorylation of p125FAK and associated proteins like paxillin and p130Cas and directly link them to cell adhesion (34). Recently, $G\alpha_{12}$ and $G\alpha_{13}$ were also shown to interact directly with cadherin and induce the release of β-catenin on activation, providing more evidence for the involvement of $G\alpha_{12}$ and $G\alpha_{13}$ in cell adhesion (52). The phenotypes observed in $G\alpha_{12}$ and $G\alpha_{13}$ doubly deficient embryos suggest an overlapping function of $G\alpha_{12}$ with $G\alpha_{13}$ during early embryogenesis. A gene-dosage effect was also observed, because at least one intact allele of both $G\alpha_{12}$ and $G\alpha_{13}$ is required to overcome the early developmental block. In contrast to the clear overlapping functions of $G\alpha_{12}$ and $G\alpha_{13}$ during mouse development, $G\alpha_{12}$ and $G\alpha_{13}$ displayed a difference in their ability to mediate receptor-dependent chemokinetic effects. Although expression of $G\alpha_{13}$ in $G\alpha_{13}$-deficient cells leads to increased migratory response, expression of $G\alpha_{12}$ does not seem to have an effect. Small G proteins, including RhoA, Rac, and Cdc42, have been implicated in the signaling processes involved in cell migration. Although both $G\alpha_{12}$ and $G\alpha_{13}$ have been shown to signal through small G proteins, especially RhoA, differences exist in the ways the signals are transmitted. For example, although both $G\alpha_{12}$ and $G\alpha_{13}$ use p115RhoGEF as GAP only activated $G\alpha_{13}$, but not activated $G\alpha_{12}$, stimulates its GEF activity (36). Thus, in our embryonic fibroblast system, $G\alpha_{12}$ does not mediate the chemokinetic response to LPA, whereas $G\alpha_{13}$ does.

$G\alpha_{12}/G\alpha_{13}$-mediated signaling pathways have also been shown to functionally interact with $G\alpha_q/G\alpha_{11}$-mediated signaling processes, most likely in a synergistic manner. For example, in platelets, thromboxane-A_2 (TXA_2) receptor-induced $G\alpha_q$ activation leads to phospholipase C-Ca^{2+}/calmodulin-dependent myosin light chain kinase activation, whereas TXA_2 receptor-induced $G\alpha_{12}/G\alpha_{13}$ activation results in activation of Rho/Rho-kinase, which further phosphorylates and inhibits myosin phosphatase. Thus, $G\alpha_q$ and $G\alpha_{12}/G\alpha_{13}$ synergistically increase myosin light chain phosphorylation in activated platelets (42, 53, 54) and possibly in a variety of other cells. Previous work in our lab with $G\alpha_q$ and $G\alpha_{11}$ double knockout mice showed that the relationship between $G\alpha_q$ and $G\alpha_{11}$ in mouse development is similar to that of $G\alpha_{12}$ and $G\alpha_{13}$. At least one intact copy of either $G\alpha_q$ or $G\alpha_{11}$ is required to bring embryos to term (55). We were interested in examining whether $G\alpha_{12}$ also interacts with the $G\alpha_q$ signaling pathway. Double heterozygous breeding shows that $G\alpha_q$ and $G\alpha_{12}$ doubly deficient animals die *in utero* at about E13 (Table 3), whereas most $G\alpha_q-/-$ embryos and almost all $G\alpha_{12}-/-$ embryos survive. These results suggest an overlapping function of $G\alpha_{12}$ with $G\alpha_q$ at a different stage of embryogenesis than the functional overlap found with $G\alpha_{13}$.

Interestingly, the gene-dosage effect between $G\alpha_{12}$ and $G\alpha_q$ differs from the gene-dosage effect between $G\alpha_{12}$ and $G\alpha_{13}$ (at least one intact allele of both $G\alpha_{12}$ and $G\alpha_{13}$ is necessary for extrauterine life), whereas at least one intact copy of either $G\alpha_q$ or $G\alpha_{12}$ is required. Although the physiological role that $G\alpha_{12}$ plays in these processes is still not clear, our results demonstrate functional overlap between $G\alpha_{12}$ and $G\alpha_{13}$ or $G\alpha_q$ during different stages of embryogenesis. Although we have not identified the processes in which each of these genes plays a dominant role, we can clearly see where their functions overlap. Extensive studies with isolated cells deficient in different G proteins will be necessary to analyze the nature of these signaling networks.

This work is supported in part by National Institutes of Health Grant AG12288 awarded (to M.I.S.). J.L.G. is the recipient of National Research Service Award postdoctoral award 5 F32 HL10496-02. S.M. is the recipient of Deutsche Forschungsgemeinschaft Grant MU 1352/1-1.

1. Simon, M. I., Strathmann, M. P. & Gautam, N. (1991) *Science* **252,** 802–808.
2. Strathmann, M. P. & Simon, M. I. (1991) *Proc. Natl. Acad. Sci. USA* **88,** 5582–5586.
3. Offermanns, S., Laugwitz, K. L., Spicher, K. & Schultz, G. (1994) *Proc. Natl. Acad. Sci. USA* **91,** 504–508.
4. Wilk-Blaszczak, M. A., Singer, W. D., Gutowski, S., Sternweis, P. C. & Belardetti, F. (1994) *Neuron* **13,** 1215–1224.
5. Aragay, A. M., Collins, L. R., Post, G. R., Watson, A. J., Feramisco, J. R., Brown, J. H. & Simon, M. I. (1995) *J. Biol. Chem.* **270,** 20073–20077.
6. Laugwitz, K. L., Allgeier, A., Offermanns, S., Spicher, K., Van Sande, J., Dumont, J. E. & Schultz, G. (1996) *Proc. Natl. Acad. Sci. USA* **93,** 116–120.
7. Barr, A. J., Brass, L. F. & Manning, D. R. (1997) *J. Biol. Chem.* **272,** 2223–2229.
8. Macrez-Lepretre, N., Kalkbrenner, F., Morel, J. L., Schultz, G. & Mironneau, J. (1997) *J. Biol. Chem.* **272,** 10095–10102.
9. Moolenaar, W. H., Kranenburg, O., Postma, F. R. & Zondag, G. C. (1997) *Curr. Opin. Cell Biol.* **9,** 168–173.
10. An, S., Goetzl, E. J. & Lee, H. (1998) *J. Cell Biochem. Suppl.* **30–31,** 147–157.
11. Kitamura, K., Shiraishi, N., Singer, W. D., Handlogten, M. E., Tomita, K. & Miller, R. T. (1999) *Am. J. Physiol.* **276,** C930–C937.
12. Xu, N., Bradley, L., Ambdukar, I. & Gutkind, J. S. (1993) *Proc. Natl. Acad. Sci. USA* **90,** 6741–6745.
13. Jiang, H., Wu, D. & Simon, M. I. (1993) *FEBS Lett.* **330,** 319–322.
14. Voyno-Yasenetskaya, T. A., Pace, A. M. & Bourne, H. R. (1994) *Oncogene* **9,** 2559–2565.
15. Prasad, M. V., Dermott, J. M., Heasley, L. E., Johnson, G. L. & Dhanasekaran, N. (1995) *J. Biol. Chem.* **270,** 18655–18659.
16. Collins, L. R., Minden, A., Karin, M. & Brown, J. H. (1996) *J. Biol. Chem.* **271,** 17349–17353.
17. Fromm, C., Coso, O. A., Montaner, S., Xu, N. & Gutkind, J. S. (1997) *Proc. Natl. Acad. Sci. USA* **94,** 10098–10103.
18. Mao, J., Yuan, H., Xie, W., Simon, M. I. & Wu, D. (1998) *J. Biol. Chem.* **273,** 27118–27123.
19. Dhanasekaran, N., Prasad, M. V., Wadsworth, S. J., Dermott, J. M. & van Rossum, G. (1994) *J. Biol. Chem.* **269,** 11802–11806.
20. Voyno-Yasenetskaya, T., Conklin, B. R., Gilbert, R. L., Hooley, R., Bourne, H. R. & Barber, D. L. (1994) *J. Biol. Chem.* **269,** 4721–4724.
21. Hooley, R., Yu, C. Y., Symons, M. & Barber, D. L. (1996) *J. Biol. Chem.* **271,** 6152–6158.
22. Lin, X., Voyno-Yasenetskaya, T. A., Hooley, R., Lin, C. Y., Orlowski, J. & Barber, D. L. (1996) *J. Biol. Chem.* **271,** 22604–22610.
23. Buhl, A. M., Johnson, N. L., Dhanasekaran, N. & Johnson, G. L. (1995) *J. Biol. Chem.* **270,** 24631–24634.
24. Katoh, H., Aoki, J., Yamaguchi, Y., Kitano, Y., Ichikawa, A. & Negishi, M. (1998) *J. Biol. Chem.* **273,** 28700–28707.
25. Wadsworth, S. J., Gebauer, G., van Rossum, G. D. & Dhanasekaran, N. (1997) *J. Biol. Chem.* **272,** 28829–28832.
26. Plonk, S. G., Park, S. K. & Exton, J. H. (1998) *J. Biol. Chem.* **273,** 4823–4826.
27. Slice, L. W., Bui, L., Mak, C. & Walsh, J. H. (2000) *Biochem. Biophys. Res. Commun.* **276,** 406–410.
28. Vara Prasad, M. V. & Dhanasekaran, N. (1999) *Oncogene* **18,** 1639–1642.
29. Hart, M. J., Jiang, X., Kozasa, T., Roscoe, W., Singer, W. D., Gilman, A. G., Sternweis, P. C. & Bollag, G. (1998) *Science* **280,** 2112–2114.
30. Fukuhara, S., Murga, C., Zohar, M., Igishi, T. & Gutkind, J. S. (1999) *J. Biol. Chem.* **274,** 5868–5879.
31. Jiang, Y., Ma, W., Wan, Y., Kozasa, T., Hattori, S. & Huang, X. Y. (1998) *Nature (London)* **395,** 808–813.

32. Gohla, A., Harhammer, R. & Schultz, G. (1998) *J. Biol. Chem.* **273,** 4653–4659.
33. Mao, J., Xie, W., Yuan, H., Simon, M. I., Mano, H. & Wu, D. (1998) *EMBO J.* **17,** 5638–5646.
34. Needham, L. K. & Rozengurt, E. (1998) *J. Biol. Chem.* **273,** 14626–14632.
35. Shi, C. S., Sinnarajah, S., Cho, H., Kozasa, T. & Kehrl, J. H. (2000) *J. Biol. Chem.* **275,** 24470–24476.
36. Kozasa, T., Jiang, X., Hart, M. J., Sternweis, P. M., Singer, W. D., Gilman, A. G., Bollag, G. & Sternweis, P. C. (1998) *Science* **280,** 2109–2111.
37. Xu, N., Voyno-Yasenetskaya, T. & Gutkind, J. S. (1994) *Biochem. Biophys. Res. Commun.* **201,** 603–609.
38. Althoefer, H., Eversole-Cire, P. & Simon, M. I. (1997) *J. Biol. Chem.* **272,** 24380–24386.
39. Berestetskaya, Y. V., Faure, M. P., Ichijo, H. & Voyno-Yasenetskaya, T. A. (1998) *J. Biol. Chem.* **273,** 27816–27823.
40. Davignon, I., Barnard, M., Gavrilova, O., Sweet, K. & Wilkie, T. M. (1996) *Genomics* **31,** 359–366.
41. Harhammer, R., Nurnberg, B., Spicher, K. & Schultz, G. (1994) *Biochem. J.* **303,** 135–140.
42. Offermanns, S., Mancino, V., Revel, J. P. & Simon, M. I. (1997) *Science* **275,** 533–536.
43. Yang, J. T., Rayburn, H. & Hynes, R. O. (1993) *Development (Cambridge, U.K.)* **119,** 1093–1105.
44. Pear, W. S., Nolan, G. P., Scott, M. L. & Baltimore, D. (1993) *Proc. Natl. Acad. Sci. USA* **90,** 8392–8396.
45. Offermanns, S., Toombs, C. F., Hu, Y. H. & Simon, M. I. (1997) *Nature (London)* **389,** 183–186.
46. George, E. L., Baldwin, H. S. & Hynes, R. O. (1997) *Blood* **90,** 3073–3081.
47. Ilic, D., Furuta, Y., Suda, T., Atsumi, T., Fujimoto, J., Ikawa, Y., Yamamoto, T. & Aizawa, S. (1995) *Biochem. Biophys. Res. Commun.* **209,** 300–309.
48. Kwee, L., Burns, D. K., Rumberger, J. M., Norton, C., Wolitzky, B., Terry, R., Lombard-Gillooly, K. M., Shuster, D. J., Kontgen, F., Stewart, C., *et al.* (1995) *Ciba Found. Symp.* **189,** 17–28.
49. Xu, W., Baribault, H. & Adamson, E. D. (1998) *Development (Cambridge, U.K.)* **125,** 327–337.
50. Zhang, Q., Magnusson, M. K. & Mosher, D. F. (1997) *Mol. Biol. Cell* **8,** 1415–1425.
51. Laudanna, C., Campbell, J. J. & Butcher, E. C. (1996) *Science* **271,** 981–983.
52. Meigs, T. E., Fields, T. A., McKee, D. D. & Casey, P. J. (2001) *Proc. Natl. Acad. Sci. USA* **98,** 519–524.
53. Klages, B., Brandt, U., Simon, M. I., Schultz, G. & Offermanns, S. (1999) *J. Cell Biol.* **144,** 745–754.
54. Offermanns, S. (2000) *Biol. Chem.* **381,** 389–396.
55. Offermanns, S., Zhao, L. P., Gohla, A., Sarosi, I., Simon, M. I. & Wilkie, T. M. (1998) *EMBO J.* **17,** 4304–4312.